

The effect of Cu substitution on the A_{1g} mode of $\text{La}_{0.7}\text{Sr}_{0.3}\text{MnO}_3$ manganites

G. De Marzi^{a,1}, H. J. Trodahl^b, J. Bok^c, A. Cantarero^a, and F. Sapiña^a

^a *Materials Science Institute, University of Valencia, PO Box 22085, 46071 Valencia, Spain*

^b *School of Chemical and Physical Sciences, Victoria University of Wellington, PO Box 600, Wellington, New Zealand*

^c *ESPCI, 10 rue Vauquelin, 75231 Paris CEDEX 05, France*

Abstract

We report on the first Raman data of Cu substituted $\text{La}_{1-y}\text{Sr}_y\text{Mn}_{1-x}\text{Cu}_x\text{O}_3$ ($0 \leq x \leq 0.10$ and $0.17 \leq y \leq 0.3$, accordingly in order to have the same $\text{Mn}^{4+}/[\text{Mn}^{4+}+\text{Mn}^{3+}]$ ratio), collected in the frequency range $100\text{-}900\text{ cm}^{-1}$ and at room temperature, with parallel ($e_i \parallel e_s$) and crossed ($e_i \perp e_s$) polarizations of the incident (e_i) and scattered (e_s) light. Spectra were fitted with a Drude-Lorentz model, and peaks at $190\text{-}220$ and 430 cm^{-1} , together with two broad structures centered at near 500 and 670 cm^{-1} , have been found. We also have observed that the A_{1g} mode is substantially shifted with increasing Cu substitution. The A_{1g} phonon shift is a linear function of the tolerance factor t and the rhombohedral angle α_r , thus following the structural changes of the MnO_6 octahedra in the system.

Key words: Raman spectroscopy, manganites, phonons

PACS: 78.30.Hv, 75.47.Ex, 63.20.Dj, 78.20.-e

1 Introduction

The intriguing physical properties and the potential technological applications of $R_{1-x}A_x\text{MnO}_3$ pseudocubic manganites (where R is a rare-earth metal: La, Pr, Nd, Dy; and A is an alkaline earth: Sr, Ca, Ba, Pb) have led to a resurgence

Email address: gdemarzi@nmrc.ie (G. De Marzi).

¹ Present address: NMRC, Lee Maltings - Prospect Row, Cork, Ireland

of interest in these and related materials. In particular, the phase diagram of these compounds is complex, and many variables such as pressure, applied magnetic field, doping concentration x , and A -site average ionic radius can determine a wide range of ground states in the system [1]. In many of these systems a metal-insulator transition (MI) and colossal magnetoresistance occur near the Curie temperature T_c , when the system undergoes a paramagnetic (PM) to ferromagnetic (FM) transition. To explain the PM to FM phase transition and the changes in transport mechanisms, Zener proposed the so-called “double exchange (DE)” model [2]. In the framework of the DE model, two carriers hop simultaneously, one from a Mn^{3+} ion to an adjacent O^{2-} site and the other from the O^{2-} to a neighboring Mn^{4+} . However, numerous experimental results suggest that other considerations influence the phase transitions, among them the electron-phonon interaction arising from Jahn-Teller (JT) distortions [3], the orbital degree of freedom [4], the electron-electron correlations and the coupling between spin and orbital structure [5]. The JT lattice distortion in particular is thought to be larger in the PM phase (above T_c), but to decrease [3] significantly after the transition to the FM phase. Thus, the MnO_6 octahedra are highly distorted for $T > T_c$ but the magnitude of this distortion decreases as T approaches T_c . The idea is that a MI transition can occur more easily if the octahedra are undistorted and the Mn–O–Mn angles tends to 180° [6,7]; this effect can also be obtained by changing the average dimension of the atom at the A and/or B site. Studies of $R_{1-x}A_xMnO_3$ with x close to 30% have shown the existence of a relationship between T_c and the distortion of the perovskite structure as measured by the tolerance factor, t , or the mean size of cations at the A site $\langle r_A \rangle$ [6,8]. More precisely, it has been shown that in perovskite series with a fixed $\langle r_A \rangle$ value, the T_c depends on the disorder at the A site [9,10]; this disorder is quantified in terms of the variance of the A cationic radii distribution, $\sigma^2(\langle r_A \rangle)$. There is substantially less information in literature regarding the substitution in the B cationic sublattice. Some attention has been paid to the substitutions on the charge ordered ground state (i.e., 50% Mn^{4+}) [11], but there are few results concerning Mn-substitution having the optimum content of Mn^{4+} (ca. 30%). There is not yet enough data to correlate the dependence of T_c with any structural variable involving B -site substitution [12]. The size of the substitutional defects is a key factor influencing transition temperatures [10]; the structural disorder produces a strong local stress in MnO_6 octahedra (resulting in a rotation), modifying the Mn–O–Mn angles and thus changing lattice and electronic properties. Thus both vibrational and electronic properties of mixed valence manganites with defect in the B cation sublattice are influenced by structural disorder introduced by local internal pressure associated to the substitutional defects. In this paper we present a Raman scattering investigation on the manganese perovskites $La_{1-y}Sr_yMn_{1-x}Cu_xO_3$ as a function of B -site Cu doping. The copper-free end member of the series, $La_{0.7}Sr_{0.3}MnO_3$ (LSMO), has been extensively studied with a great variety of techniques; for spectroscopic spectra, see for example optical conductivity measurements [13,14,15],

and Raman scattering [16,17,18,19]. Nevertheless, reflectivity, Raman and/or ellipsometric studies have not been yet performed on $\text{La}_{1-y}\text{Sr}_y\text{Mn}_{1-x}\text{Cu}_x\text{O}_3$. In this paper we report a Raman study of a series containing a fixed ratio $\text{Mn}^{4+}/(\text{Mn}^{4+}+\text{Mn}^{3+}) = 0.3$.

2 Experiment

Substitution in specific sites in the lattice affects the vibrational modes through changes to the mass, the bonding strength and the bonding configuration, so that Raman spectroscopy and infrared (reflectance and ellipsometry techniques) are ideal tools for studying the role of *B*-site substitution in manganites. Moreover, Raman spectroscopy is a useful probe for those materials in which lattice, as well as electron dynamics, strongly interacts by means of electron-phonon interaction. With this in mind we have measured Raman spectra of polycrystalline $\text{La}_{1-y}\text{Sr}_y\text{Mn}_{1-x}\text{Cu}_x\text{O}_3$ samples, searching for effects due to the changes in both electron-phonon coupling and free carrier screening in the metallic phase. As an ease to interpretation the values of *y* are selected to keep constant the ratio $\text{Mn}^{4+}/(\text{Mn}^{4+}+\text{Mn}^{3+}) = 0.3$ through the series. Details on the preparation of the studied samples, together with x-ray diffraction and magnetization measurements are described elsewhere [10], while values of *y* and Cu content, T_c temperature, tolerance factor, and rhombohedral angle are given in Table I. Raman spectra were collected at room temperature with back-scattering geometry of the incident laser light from surfaces polished down to 1 μm with diamond paste. The samples were excited with the 514.5 nm line of a Ar ion laser and the scattered light analyzed using a triple monochromator system (DILOR XY800) with a LN_2 cooled Charge-Coupled device (CCD) detector. The power was kept below 15 mW focused in a spot diameter of 0.1 mm^2 , in order to avoid heating the samples. Spectra were collected with parallel ($e_i \parallel e_s$) and crossed ($e_i \perp e_s$) polarizations of the incident (e_i) and scattered (e_s) light. In Figs. 1 and 2, respectively, the Raman spectra collected in the parallel-polarized and cross-polarized configurations are shown.

3 Results and discussion

As in the case of previously published spectra for $\text{La}_{0.7}\text{Sr}_{0.3}\text{MnO}_3$ [18,19], and many related materials [20], the most striking features are two anomalously broad lines centered near 500 and 670 cm^{-1} . In addition to these very broad structures, there are narrower lines at 190-220 and 430 cm^{-1} . It should be noticed that the shoulder at around 600 cm^{-1} disappears for $x = 0$. In the

cross polarized configuration, the first peak at about 200 cm^{-1} completely disappears. The Raman spectra showed in Fig. 1 were fitted in the $130\text{-}900 \text{ cm}^{-1}$ region frequency with the following expression for the Raman intensity [21]:

$$S(\omega) = \frac{A(\Gamma/2)^2}{\omega^2 + (\Gamma/2)^2} + \sum_{i=1}^5 \frac{A_i \omega_i \omega \gamma_i^2}{(\omega^2 - \omega_i^2)^2 + (\omega \gamma_i)^2} \quad , \quad (1)$$

where the first term represents the electronic contribution to the spectrum, consisting of “collision-dominated” low-frequency response associated with diffusive hopping of the carriers. The second term represents the “odd lorentzian” shape of a phonon mode (ω_i , γ_i , and A_i are the peak frequency, linewidth, and amplitude, respectively). The error on the frequency resulting from the fit analysis is always smaller than the resolution of the spectrometer (1.5 cm^{-1} when the aperture of the slit is $200 \mu\text{m}$). Therefore, we assume that the error is 1.5 cm^{-1} for all the frequencies. We found four peaks at $180\text{-}215$, 430 , 530 , and 670 cm^{-1} . Note that a high frequency oscillator (near 1100 cm^{-1}) is necessary to achieve a good fit. It should be pointed out that this High Frequency Contribution (HFC) is also found in Raman experiments on $\text{La}_{0.75}\text{Ca}_{0.25}\text{MnO}_3$ [22], and it has been suggested that the HFC should be associated with the photoionization of small polarons. But we argue that this is a very clear evidence that the feature up there is second order phonon scattering. In fact, the HFC structure is also present in Sr doped manganites, and all other pseudocubic and double layer manganites [22,23] and we believe that such features are weak second-order Raman scattering effects (density of state), mirroring the bands seen in the region $400\text{-}800 \text{ cm}^{-1}$. The frequencies of the experimental peaks are plotted in Fig. 3, wherein it is evident that the narrow lower peak shows a substantial shift as function of Cu concentration. Our samples exhibit rhombohedral crystal structure [10], space group $D_{3d}^6(R\bar{3}c)$. According to site group analysis, 30 vibrational modes are predicted:

$$\Gamma(D_{3d}^6) = 2A_{1u} + 3A_{2g} + A_{1g} + 4A_{2u} + 4E_g + 6E_u \quad , \quad (2)$$

where the $A_{1g} + 4E_g$ modes are Raman active, the $3A_{2u} + 5E_u$ are infrared active, and the $A_{1u} + 3A_{2g}$ are silent modes. Following the procedure described in Ref. [24], the La (or Sr) ions participate in four phonon modes ($A_{2g} + A_{2u} + E_g + E_u$), the Mn (or Cu) ions take part in four phonon modes ($A_{1u} + A_{2u} + 2E_u$), while the oxygen ions contribute in twelve modes ($A_{1g} + A_{1u} + 2A_{2g} + 2A_{2u} + 3E_g + 3E_u$). As a consequence, it is found that the A_{1g} modes only involve the motion of the oxygen ions in the C_2 sites, while the E_g arise both from oxygen site and La (Sr) site vibrations. Following Granado *et al.* [19], we assign the lowest frequency peak at $190\text{-}220 \text{ cm}^{-1}$ (M1) to an A_{1g} mode, and the peak at 430 cm^{-1} (M2) to a E_g symmetry. The assignment of the M1 peak to an A_{1g} mode is confirmed by the fact that this mode is absent in cross polarized configuration, as it is expected under these conditions (we remind the selection

rules for this mode: $A_{1g} \rightarrow \alpha_{xx} + \alpha_{yy}, \alpha_{zz}$, see Ref. [24]). Concerning the peaks at 530 cm^{-1} (M3) and 670 cm^{-1} (M4), Granado *et al.* suggest that the M3 and M4 peaks should be due to scattering induced by orthorhombic distortions which may be present on the surface. On the other hand these modes are very broad in all manganites, which is an evidence that they are full-band modes, rendered Raman active by disordered Jahn-Teller distortions [20,23]. The M1 mode corresponds to a rotation of the octahedra around the hexagonal *c*-axis [19], which is closely related with the A_g mode in the orthorhombic (*Pnma*) structure [18] (an *in-phase rotation* of the MnO_6 octahedra around the *b*-axis). Concerning the frequency shift of the A_{1g} mode, this does not simply involve the motion of the La (Sr) ions: in fact, in such a case the frequency should decrease as the heavier La ions are substituted for Sr (see the values for *y* in Table I): actually, what is seen is exactly the opposite behavior. It is worth noting that, according with the site group analysis previously discussed, the A_{1g} mode involves only the motion of the oxygen ions in the C_2 sites. Therefore it is reasonable to relate the changes on the A_{1g} mode frequency to the modifications of the oxygen octahedra. Moreover, the introduction of substitutional defect in the *B*-site (like Cu) has a strong effect in the structural changes of the lattice. Since Cu substitution induces a strong local stress, it can be expected that MnO_6 octahedra rotate, and the Mn-O bond lengths decrease under this compression. Also the Sr substitution may introduce structural disorder, but it should be noticed that, since the Sr and La ions have similar radii, the strength of the distortion induced by those ions is less important. In conclusion, we believe that the observed frequency shift with doping is determined by the distortions introduced by the large substitutional Cu ions, involving the motion of the oxygen cages and an effective rotation of the octahedra. In order to be more quantitatively, let us discuss the tolerance factor (*t*), which is defined as:

$$t = \frac{d_{A-O}}{\sqrt{2}d_{B-O}} = \frac{\langle r_A \rangle + r_O}{\sqrt{2}(\langle r_B \rangle + r_O)} \quad , \quad (3)$$

where *d* denotes the interatomic distance simply calculated as the sum of ionic medium radii; $\langle r_A \rangle$ is the average ionic radius of *A*-site ions (La^{3+} and Sr^{3+}) and $\langle r_B \rangle$ is the average radius of the *B*-site ions (Mn and Cu). The tolerance factors is $t = 1$ for spherical ions packed in the ideal perovskite structure (Mn–O–Mn angle equal to 180° , and no-tilt of the octahedra) and becomes smaller as $\langle r_B \rangle$ is increased by Cu substitution and the lattice becomes more distorted; this means that the Mn–O–Mn angle deviates from 180° , which leads to a reduction of the DE mechanism. The correlation between the frequency shift of the A_{1g} mode and the tolerance factor (calculated using the Shannon radii [25]) is shown in Fig. 4. Within the errors, it can be concluded that the scaling of the A_{1g} mode with the tolerance factor is linear. It is important to notice that the changes in the tolerance factor have been induced by both

A- and B-site substitution; in literature, there is substantial previous Raman data on the manganites as a function of A-site substitution: an interesting work by Amelichev *et al.* [18] showed that the band shift of the A_{1g} mode is a linear function of the tolerance factor for a fixed value of x (like 0.3 or 0.45). In their work, the tolerance factor is changed by introducing different cations (La, Nd, Sr, Ca, Pr, Sm, Eu, Gd) in the A sublattice of the perovskite structure. In order to compare the effect of A-site and both A- and B-site substitutions, we have added in Fig.4 their results for $R_{0.7}A_{0.3}MnO_3$ ($R = La_{1-x}Pr_x$, $A = Ca, Sr, Sr_{0.5}Ca_{0.5}$), $R_{0.67}Sr_{0.33}MnO_3$ ($R = Nd_{0.5}Sm_{0.5}, Sm, Eu, Gd$), and $R_{0.55}Sr_{0.45}MnO_3$ ($R = Nd, Nd_{0.5}Sm_{0.5}, Sm, Eu, Gd$). The solid lines are a linear fitting of $R_{0.7}A_{0.3}MnO_3$ ($\omega = 2975-2995 \cdot t$) and $R_{0.55}Sr_{0.45}MnO_3$ ($\omega = 3088 - 3092 \cdot t$) [18]. Our data are in good agreement with the $R_{0.7}A_{0.3}MnO_3$ series; in our case, $\omega = 2853 - 2864 \cdot t$, and linear extrapolations to higher t suggest that the mode should soften to zero at $t = 0.996$ ($t = 0.993$ and $t = 1.001$ for $R_{0.7}A_{0.3}MnO_3$ and $R_{0.55}A_{0.45}MnO_3$). In facts, the linear scaling of the A_{1g} mode with tolerance factor is independent of the means by which the tolerance factor is changed, as long as the Mn^{3+}/Mn^{4+} ratio is kept at a fixed value. Moreover, it is worth noting that the frequency of the A_{1g} mode can also be correlated with the rhombohedral angle α_r , whose deviation from 60° defines a measure of the rhombohedral distortion with respect to the ideal cubic structure. The values for α_r have been obtained from x-ray diffraction data, and are reported in Table I. The linear relationship between the frequency shift of the A_{1g} mode and α_r is shown in the inset of Fig. 4. It can be concluded that the band shift is a linear function of the tolerance factor and the rhombohedral angle α_r , that is, the A_{1g} mode follows the structural changes of the oxygen cages.

4 Conclusions

Our experimental studies of the Raman spectra of $La_{1-y}Sr_yMn_{1-x}Cu_xO_3$ reveal that two strong peaks appear at $190-220$ and 430 cm^{-1} , together with two broad structures centered at near 500 and 670 cm^{-1} . It is found that the lowest peak (assigned as an A_{1g} mode) shifts linearly, with the increase of Cu concentration, toward higher frequencies as x increase. Within an analysis in terms of tolerance factor and of rhombohedral angle (α_r) of the $D_{3d}^6(R_{3c})$ structure, it is proved that the shift is determined by the structural disorder introduced by substitutional Cu ions in the B -site, e.g., the shift follows the changes of the MnO_6 octahedra in the system.

Finally, it should be pointed out that the structural distortions can be influenced by the size of the B-site ion. According to the Shannon radii (r_M), the Cu ionic radius ($r_{Cu^{2+}} = 0.730$) is relatively large compared to the Mn radius ($r_{Mn^{3+}} = 0.645$, $r_{Mn^{4+}} = 0.530$); in contrast, ions such Cr^{3+} , Co^{3+} ,

Ga^{3+} ($r_{\text{Cr}^{3+}} = 0.615$, $r_{\text{Co}^{3+}} = 0.610$, $r_{\text{Ga}^{3+}} = 0.620$) are similar to the Mn mean ionic radius ($r_{\langle \text{Mn} \rangle} = 0.611$, calculated for a mean oxidation state of 3). Therefore, Raman measurements on (La,Sr) MnO_3 systems with smaller B-site substitutional defect (such as Cr^{3+} , Co^{3+} , Ga^{3+}) are highly desirable: according to our interpretation, in this case the phonon frequency shift should be less pronounced.

5 Acknowledgements

The authors would like to thank Prof. N. Joshi, Dr. S. Lupi and Dr. A. M. Power for useful discussion. This work was supported by the UE through a RTN grant (HPRN-CT2000-00021).

References

- [1] A. J. Millis, *Nature* **392**, 147 (1998); J. Fontcuberta, *Phys. World* **12**, 33 (1999).
- [2] Z. Zener, *Phys. Rev.* **82**, 403 (1951).
- [3] A. J. Millis, P. B. Littlewood, and B. I. Shraiman, *Phys. Rev. Lett.* **74**, 5144 (1995).
- [4] R. Maezono, S. Ishihara, and N. Nagaosa, *Phys. Rev. B* **57**, R13993 (1998).
- [5] S. Ishihara, J. Inoue, and S. Maekawa, *Phys. Rev. B* **55**, 8280 (1997).
- [6] H. Y. Hwang, S-W. Cheong, P. G. Radaelli, M. Marezio, and B. Batlogg, *Phys. Rev. Lett.* **75**, 914 (1995).
- [7] J. L. García-Muñoz, M. Suaaidi, J. Fontcuberta, and J. Rodríguez-Carvajal, *Phys. Rev. B* **55**, 34 (1997).
- [8] A. Maignan, V. Caignert, Ch. Simon, M. Hervieu, and B. Raveau, *J. Mater. Chem.* **5**, 1091 (1995); R. Mahesh, R. Mahendrian, A. K. Raychaudhuri, and C. N. R. Rao, *J. of Solid State Chem.* **120**, 204 (1995); J. Fontcuberta, B. Martínez, A. Seffar, S. Piñol, J. L. García-Muñoz, and X. Obradors, *Phys. Rev. Lett.* **76**, 1122 (1996).
- [9] L. M. Rodríguez-Martínez, and J. P. Attfield, *Phys. Rev. B* **54**, R15622 (1996); L. M. Rodríguez-Martínez, and J. P. Attfield, *Phys. Rev. B* **58**, 2426 (1998); J. P. Attfield, *Chem. Mater.* **10**, 3239 (1998).
- [10] Z. El-Fadli, M. Redouane Metni, F. Sapiña, E. Martínez, J.-V. Folgado, and A. Beltrán, *Chem. Mat.* **14**, 688 (2002).
- [11] A. Maignan, F. Damay, A. Barnabe, C. Martin, M. Hervieu, and B. Raveau, *Phylos. Trans. R. Soc. A* **356**, 1635 (1998), and references therein.
- [12] N. Gayathri, A. K. Raychaudhuri, S. K. Tiwary, R. Gundakaram, A. Arulraj, and C. N. R. Rao, *Phys. Rev. B* **56**, 1345 (1997); M. Rubinstein, D. J. Gillespie, J. E. Snyder, and T. M. Tritt, *Phys. Rev. B* **56**, 5412 (1997); J. Blasco, J. García, J. M. de Teresa, M. R. Ibarra, J. Perez, P. A. Algarabel, C. Marquina, and C. Ritter, *Phys. Rev. B* **55**, 8905 (1997); J. J. Blanco, L. Lezama, M. Insausti, J. Gutiérrez, J. M. Barandiarán, and T. Rojo, *Chem. Mater.* **11**, 3463 (1999); J. Gutiérrez, A. Peña, J. M. Barandiarán, J. L. Pizarro, T. Hernández, L. Lezama, M. Insausti, and T. Rojo, *Phys. Rev. B* **61**, 9028 (2000); J. Gutiérrez, A. Peña, J. M. Barandiarán, J. L. Pizarro, L. Lezama, M. Insausti, and T. Rojo, *J. Of Phys.: Condens. Matter* **12**, 10523 (2000).
- [13] Y. Okimoto, T. Katsufuji, T. Ishikawa, T. Arima, and Y. Tokura, *Phys. Rev. B* **55**, 4206 (1997).
- [14] M. Quijada, J. Černe, J. R. Simpson, H. D. Drew, K. H. Ahn, A. J. Millis, R. Shreekala, R. Ramesh, M. Rajeswari, and T. Venkatesan, *Phys. Rev. B* **58**, 16093 (1998).

- [15] K. Takenaka, K. Iida, Y. Sawaki, S. Sugai, Y. Morimoto, and A. Nakamura, *J. of Phys. Soc. of Japan* **68**, 1828 (1999).
- [16] R. Gupta, A. K. Sood, R. Mahesh, and C. N. R. Rao, *Phys. Rev. B* **54**, 14899 (1996).
- [17] V. B. Podobedov, A. Weber, D. B. Romero, J. P. Rice, and H. D. Drew, *Phys. Rev. B* **58**, 43 (1998).
- [18] V. A. Amelichev, B. Güttler, O. Yu. Gorbenko, A. R. Kaul, A. A. Bosak, and A. Yu. Ganin, *Phys. Rev. B* **63**, 104430 (2001).
- [19] E. Granado, N. O. Moreno, A. García, J. A. Sanjurjo, C. Rettori, I. Torriani, S. B. Oseroff, J. J. Neumeier, K. J. McClellan, S-W. Cheong, and Y. Tokura, *Phys. Rev. B* **58**, 11435 (1998).
- [20] A. E. Pantoja, H. J. Trodahl, A. Fainstein, R. G. Pregliasco, R. G. Buckley, G. Balakrishnan, M. R. Lees, and D. Mck. Paul, *Phys. Rev. B* **63**, 132406 (2001).
- [21] S. Yoon, H. L. Liu, G. Schollerer, S. L. Cooper, P. D. Han, D. A. Payne, S-W. Cheong, and Z. Fisk, *Phys. Rev. B* **58**, 2795 (1998).
- [22] A. Congeduti, P. Postorino, E. Caramagno, M. Nardone, A. Kumar, and D. D. Sarma, *Phys. Rev. Lett.* **86**, 1251 (2001).
- [23] A. E. Pantoja, H. J. Trodahl, R. G. Buckley, Y. Tomioka, and Y. Tokura, *J. Phys.: Cond. Matter* **13**, 3741, (2001).
- [24] D. L. Rousseau, R. P. Bauman, and S. P. S. Porto, *J. of Raman Spectroscopy* **10**, 253 (1981).
- [25] R. D. Shannon, and C. T. Prewitt, *Phys. Chem. Earth* **21**, 18 (1981).

Cu content	y doping	T_c	tolerance factor	α_r
0.00	0.300	372	0.929983	60.42202
0.02	0.274	358	0.928021	60.45980
0.04	0.248	331	0.926063	60.50238
0.06	0.222	308	0.924109	60.55491
0.08	0.196	274	0.922160	60.59863
0.10	0.170	236	0.920216	60.64173

Table 1

Chemical analysis, observed T_c (K), tolerance factor, and rhombohedral angles α_r (degrees), for samples of nominal composition $\text{La}_{1-y}\text{Sr}_y\text{Mn}_{1-x}\text{Cu}_x\text{O}_3$.

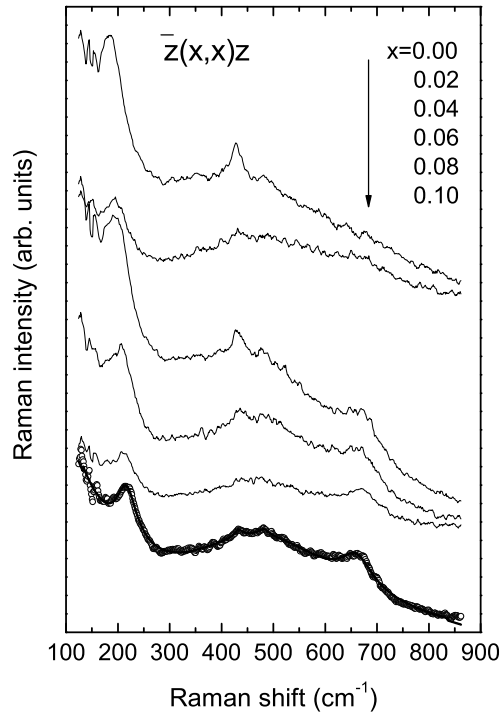


Fig. 1. Room temperature Raman spectra in parallel polarized geometry for polycrystalline $\text{La}_{1-y}\text{Sr}_y\text{Mn}_{1-x}\text{Cu}_x\text{O}_3$ samples. The solid line represents the fitting to Eq.1.

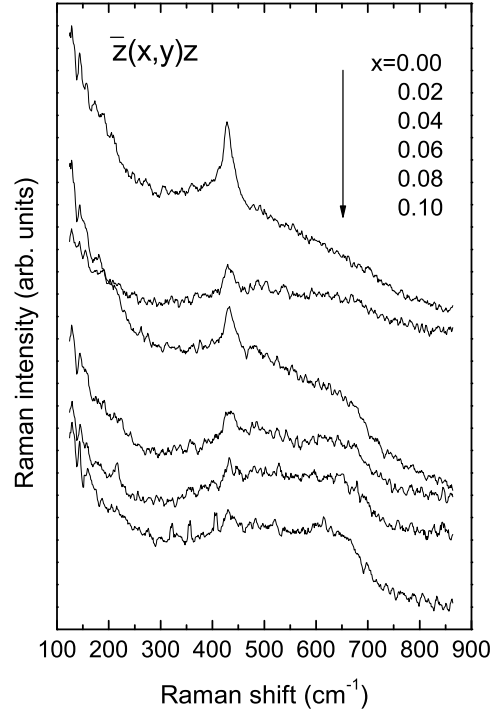


Fig. 2. Room temperature Raman spectra in cross polarized geometry for polycrystalline $\text{La}_{1-y}\text{Sr}_y\text{Mn}_{1-x}\text{Cu}_x\text{O}_3$ samples.

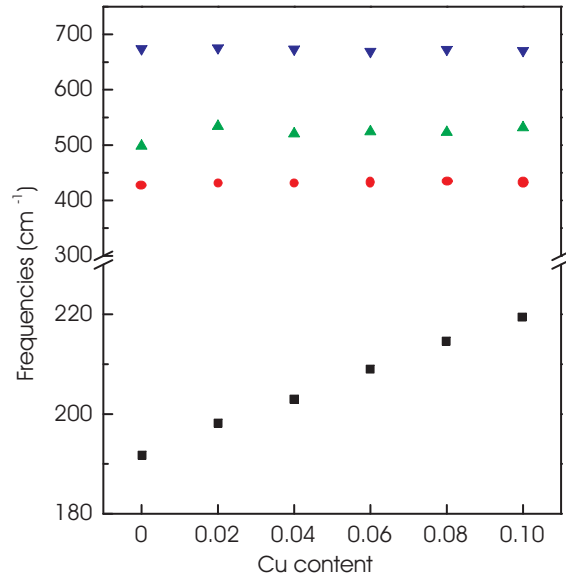


Fig. 3. *B*-site doping dependence of the four Raman shift peaks, as obtained by Eq. (1).

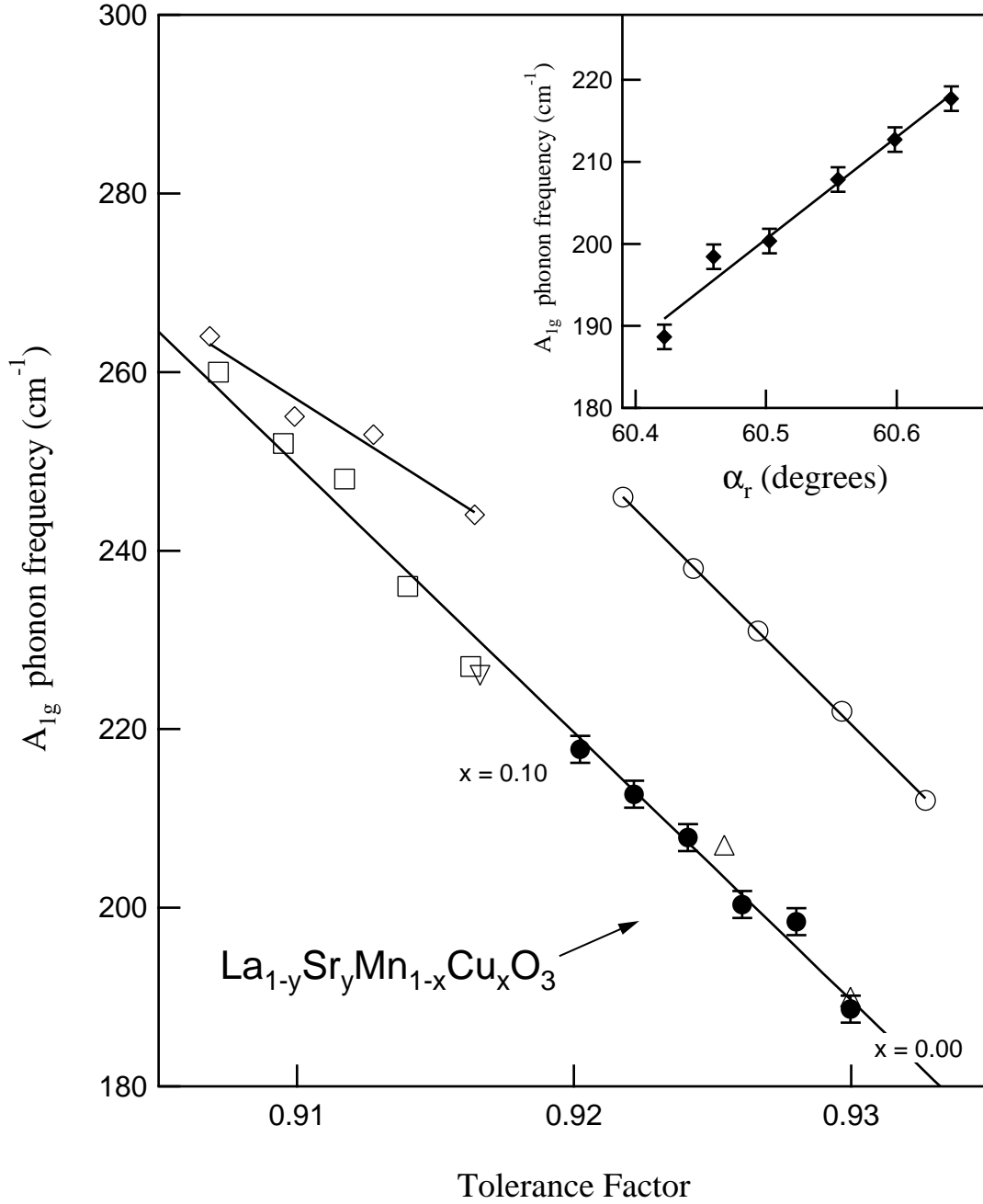


Fig. 4. Plot of the A_{1g} frequency shift as a function of the tolerance factor t for $\text{La}_{1-y}\text{Sr}_y\text{Cu}_x\text{Mn}_{1-x}\text{O}_3$ (filled circles). The following data from ref.18 are also shown in the figure: $\text{La}_{1-x}\text{Pr}_x\text{Ca}_{0.3}\text{MnO}_3$ (\square ; $x = 0, 0.25, 0.5, 0.75, 1$), $\text{La}_{1-x}\text{Pr}_x\text{Sr}_{0.3}\text{MnO}_3$ (\triangle ; $x = 0, 0.5$), $(\text{La}_{0.5}\text{Nd}_{0.5})_{0.7}(\text{Sr}_{0.5}\text{Ca}_{0.5})_{0.3}\text{MnO}_3$ (∇), $\text{R}_{0.67}\text{Sr}_{0.33}\text{MnO}_3$ (\diamond ; $\text{R} = \text{Nd}_{0.5}\text{Sm}_{0.5}, \text{Sm}, \text{Eu}, \text{Gd}$), and $\text{R}_{0.55}\text{Sr}_{0.45}\text{MnO}_3$ (\circ ; $\text{R} = \text{Nd}, \text{Nd}_{0.5}\text{Sm}_{0.5}, \text{Sm}, \text{Eu}, \text{Gd}$). The solid lines are a linear fitting of $\text{R}_{0.7}\text{A}_{0.3}\text{MnO}_3$ ($\omega = 2975-2995 \cdot t$) and $\text{R}_{0.55}\text{Sr}_{0.45}\text{MnO}_3$ ($\omega = 3088-3092 \cdot t$)[18]. A linear fit to our data (not shown in the figure) gives $\omega = 2853-2864 \cdot t$. In the inset, the A_{1g} frequency shift is plotted as function of the rhombohedral angle α_r .